Lasers in Manufacturing Conference 2023

Advanced oscillation modes in laser welding

Hana Šebestová[a,*], Petr Horník[a], Zdeněk Chlup[b], Michal Jambor[b], Zdeněk Joska[c], Libor Mrňa[a]

[a]Institute of Scientific Instruments of the Czech Academy of Sciences, Královopolská 147, 612 00 Brno, Czech Republic
[b]Institute of Physics of Materials of the Czech Academy of Sciences, Žižkova 513/22, 616 00 Brno, Czech Republic
[c]University of Defence, Faculty of Military Technology, Kounicova 65, 662 10 Brno, Czech Republic

Abstract

Modern wobble laser welding heads allow a great degree of freedom in the choice of oscillation modes resulting from a superposition of two orthogonal sinusoidal functions. Yet the basic oscillation modes like circular or transversal linear mode are still the most popular in practice. Therefore, unusual oscillation modes with more complex laser spot trajectories were suggested and experimentally achieved. In this way, wavy welds were created into martensitic 22MnB5 steel. The intention was to achieve welds with variable cross-sections, yet with a continuous root. The microstructure and properties of welds were analyzed with emphasis on changes in the heat-affected zone. We aim to provide a deeper understanding of advanced oscillation modes and their impact on the resulting weld quality and mechanical properties.

Keywords: Laser welding; beam oscillation; advanced oscillation mode; weld macrostructure; ultimate tensile strength

1. Introduction

Laser welding has evolved as a highly versatile and efficient technique for joining various materials in diverse industrial applications. The introduction of modern laser welding wobble heads has enabled a remarkable level of freedom in selecting oscillation modes by combining two orthogonal sinusoidal functions. The utilization of oscillation modes has garnered significant attention due to their potential to enhance weld quality, improve process stability, and broaden the range of applicable materials.

* Corresponding author. Tel.: +420 541 514 338.
E-mail address: sebestova@isibrno.cz.

The most common oscillation modes are line, circle, eight, or infinity. All these modes have a very similar distribution of power density across the weld leading to about a rectangular weld metal with possible side roots at high oscillation diameters (Hao et al., 2015, Horník et al., 2022, Jiang et al. 2020, Yan et al., 2022). While the basic oscillation modes remain popular in practice, the potential of advanced oscillation modes remains largely unexplored.

This article dives into the exploration and analysis of advanced oscillation modes in laser welding, investigating their characteristics, and effects on the welding process. In addition, a wobbling technique is known to reduce pores and spatters and increase overall process stability. Welds made with beam oscillation are compared with the conventional laser weld and laser weld made with a defocused beam.

We propose the unconventional oscillation modes to reach a wide wavy weld metal (WM) with continuous full penetration along the weld axis, and with a narrow either a wavy or a straight heat-affected zone (HAZ). The highest power density should be present in the weld axis to ensure deep weld and root creation, whereas the weld head should be wider with desired wavy structure. These requirements allow complex welds to be performed even with relatively low laser power and more importantly ensure lower heat input.

Visualizing the resulting laser spot trajectories and understanding the influence of oscillation parameters on these complex modes pose significant challenges. The complex beam trajectories associated with advanced oscillation modes necessitate a comprehensive analysis and understanding to effectively utilize them in practical applications.

Rapid heating and cooling rates during welding can cause changes in the microstructure of the thermo-mechanically processed steel. The heat-affected zone (HAZ) adjacent to the weld can experience a range of metallurgical transformations, including grain growth, phase transformations, and precipitation of undesirable phases. These changes can result in a loss of mechanical properties, such as reduced strength, hardness, and fatigue resistance. Additionally, residual stresses can be induced in the welded region. The assumption is that wavy beads could help reduce some of the negative effects. Therefore, this research aims to evaluate the effect of the size and shape of WM and HAZ on the mechanical properties of the welds.

2. Experiment

The IPG fiber laser YLS-2000 with a maximum output power of 2 kW was used for 22MnB5 butt welding experiments. The optical fiber with a diameter of 100 µm delivered the laser beam into the IPG wobbling head FLW-D30-W mounted on the arm of the ABB robot IRB 2400. The focused beam reached a diameter of 0.2 mm on the sheet surface. The welding speed of 20 $mm \cdot s^{-1}$ was constant for all welds. The welding was carried out in a protective argon atmosphere. The applied processing parameters are summarized in Table 1.

Table 1. Welding parameters

Beam	Beam diameter (mm)	Laser power (W)	Oscillation mode	Oscillation diameter (mm)	Oscillation frequency (Hz)
focused	0.2	1300	-	-	-
oscillating	0.2	1300	atom	4	100
oscillating	0.2	1300	fin	4	30
oscillating	0.2	1300	slinky	4	50
defocused	3	2000	-	-	-

The first weld was made without beam oscillation, and then three advanced oscillation modes (atom, fin, and slinky) were tested. Finally, a laser weld with the beam defocused to 3 mm on the material surface was made with the maximal laser power. The power density of the defocused beam was sufficient only for about half-sheet penetration even at maximal laser power. Therefore, the weld was made as a double-sided joint.

The velocity of the laser spot moving along the static trajectory of oscillation mode sums with the vector of the welding speed, and the spot trajectory is created. Fig. 1 presents the static trajectories of the modes, corresponding beam trajectories, and actual spot speed with respect to the welding speed and oscillation parameters. The modes were designed to achieve a wavy weld bead with maximal penetration in the middle of the weld width and continuous along the whole length.

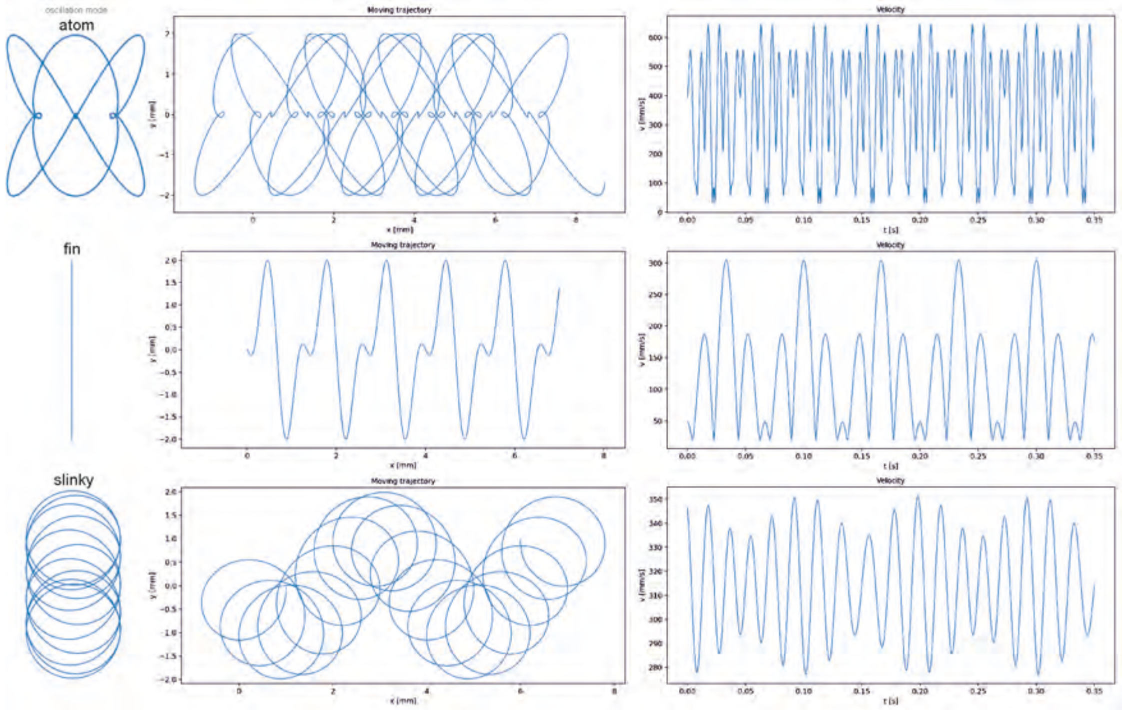

Fig. 1. Applied oscillation modes, corresponding beam trajectories, and spot speed on the material surface

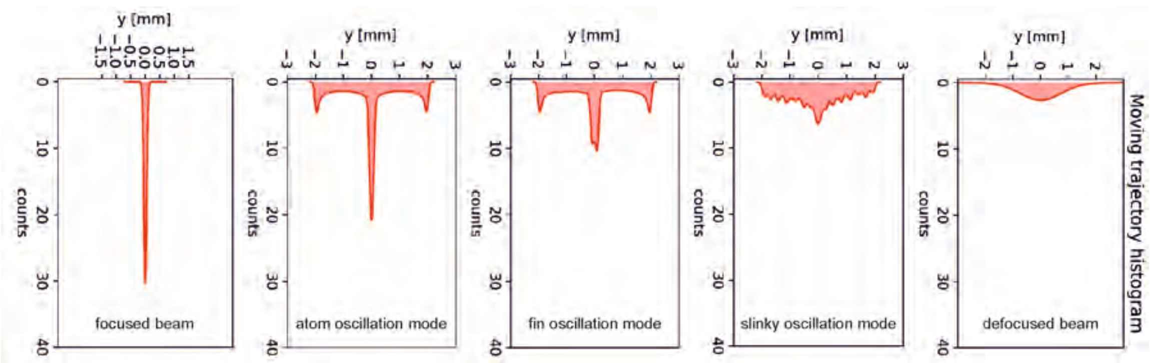

Fig. 2. Histograms of laser spot trajectory for individual welds

The histogram of the laser spot trajectory represents the average power density distribution across the weld. The histograms of experimental welds were calculated according to Horník et al., 2022 (Fig. 2). It is important to note that the welds made with beam oscillation may be inconsistent in length at low oscillation frequencies. Therefore, the individual cross-sections can have a different appearance with respect to their positions and must be calculated from a shorter section. However, the central maximum is preserved.

2.1. Materials and methods of weld inspection

The 1.5 mm thin metal sheets of press-hardenable steel 22MnB5 (trade name Usibor 1500) with Al-Si coating (150 $g \cdot m^{-2}$) were in hot-stamped condition. The coating was locally mechanically removed to eliminate ferrite formation, and the sheets were butt welded.

The welds were cut perpendicularly to the welding direction and metallographic specimens of weld cross-sections were prepared. The specimens were etched with 4% nital for 3 s to reveal the structure. Similarly, the metallographic specimens of weld surfaces were prepared. The macro- and microstructure of weld metal were observed with Keyence laser scanning confocal microscope VK-X Series 3D.

The tensile characteristics were measured according to the ISO 6892-1 standard on specimens with a cross-section of 1.5 mm × 11.5 mm welded in the middle of the parallel length. A universal testing machine Zwick/Roell Z50 with a Multisens contact extensometer was used. The specimen parallel length was 220 mm and the gauge length used for the extensometer was 90 mm. The pre-load of 100 N was applied and a crosshead speed of 2 $mm \cdot min^{-1}$ was used for the load application.

The LECO AMH 55 hardness tester was used to evaluate the Vickers microhardness according to the ISO 6507-1 and ISO 9015-2 standards. The load of 50 gf (0.5 N) and the dwell time of 12 s were applied. The measurement across each weld was performed 0.2 mm under the surface. The indents were spaced 0.08 mm.

3. Experimental results & Discussion

3.1. Weld macrostructure

Fig. 3 presents the surfaces and cross-sections of welds. In the case of beam oscillation, the welds are not homogeneous along the weld length. Thus, only an example of a possible cross-section macrostructure is shown. The fusion line is poorly visible on the weld cross-section because of the very similar microstructure of the WM and the neighboring part of the HAZ. What is more, the original WM can be re-melted or heat-affected by subsequent passes of the beam in case of beam oscillations.

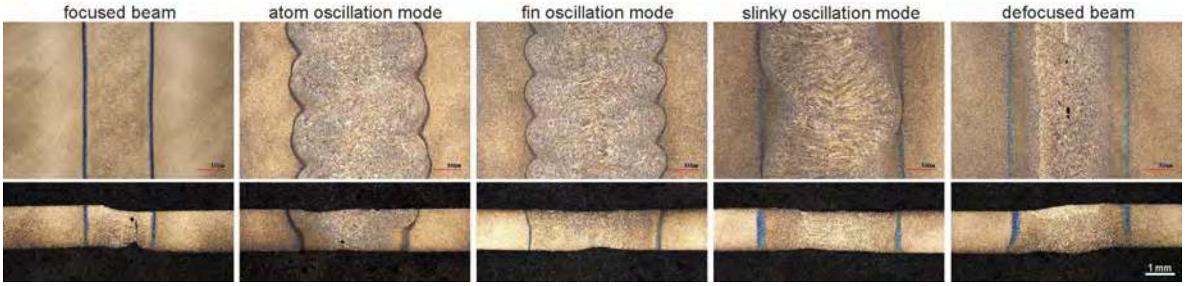

Fig. 3. The surfaces (upper) and the cross-sections (lower) of individual welds

The weld made with the focused beam has narrow both WM and HAZ. However, the keyhole was not stable during the welding because of excessive heat input. The gas escaping from the keyhole is trapped in the rapidly solidifying WM and the pore is formed. The large volume of the melt pool caused the root undercut. Moreover, the crack initiated in the fusion line close to the pore and propagated in the HAZ.

The width of the weld made with the defocused beam is more than doubled compared to the focused beam weld. The first side weld is heat affected by the second one.

The width of the wavy WM on the face side of welds made with beam oscillation is 0.2–0.4 mm higher than the oscillation diameter. The HAZ contours the shape of WM on the face side of welds made with atom and fin oscillation mode having a width of only 0.1–0.2 mm. The HAZ width increases with depth and exceeds the width of the HAZ of the weld made with the defocused beam. On the other hand, the slinky oscillation mode has almost straight HAZ having a width of about 0.25 mm on the outer radius, and up to 1.5 mm on the inner side affected by more passes of the beam. The penetration depth of the fin and slinky oscillation mode is more consistent in the weld cross-section compared to the atom oscillation mode because the spot speed fluctuates in a much narrower interval (Fig. 1).

Linear misalignment is a very common defect in thin sheet welding. The beam oscillations provide a wider WM and thus the transition between the sheets is more fluent with a lower risk of sharp notches.

3.2. Weld metal microstructure

Fig. 4 presents the microstructure of BM and the microstructure of WMs of individual welds detected in the weld center. Although the Al-Si coating was removed before welding, a certain portion of its elements already diffused into the base metal during the hot stamping. Both Si and Al are strong ferrite-stabilizes shifting both the ferrite and bainite start curve to shorter times (Gomez et al., 2009). Therefore, the microstructure is rather bainitic-martensitic than martensitic, especially at lower cooling rates.

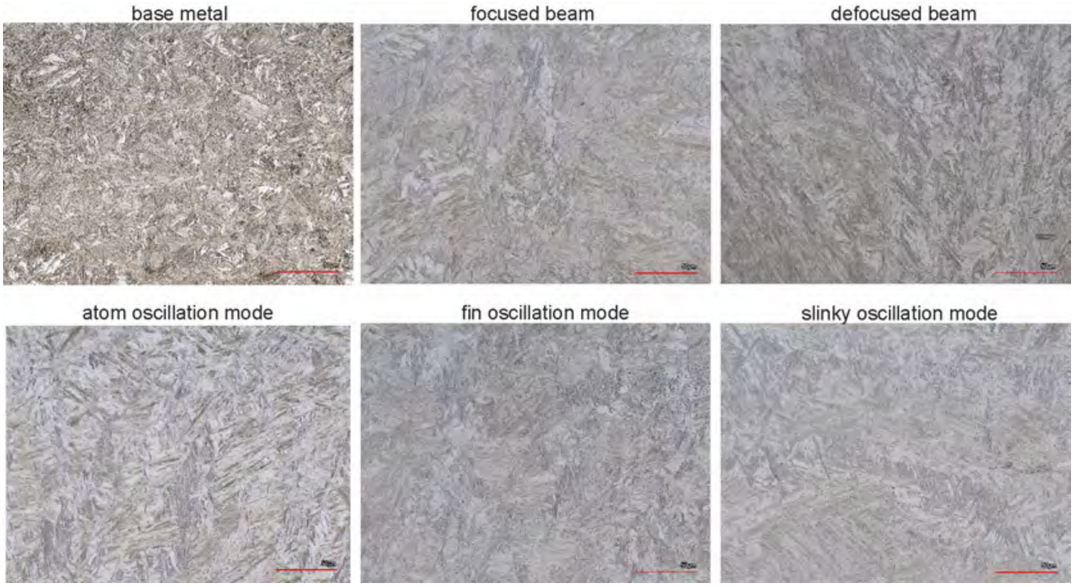

Fig. 4. Base metal and weld metal microstructure, scale 50 µm

Local segregations of Al and Si lead to the formation of ferritic regions in the WM that support the formation of cracks and thus weaken the weld joint. They were observed in both welds made without beam oscillation (Fig. 5). The portion of ferrite in the weld metal is higher when coated sheets are welded (Šebestová et al., 2021).

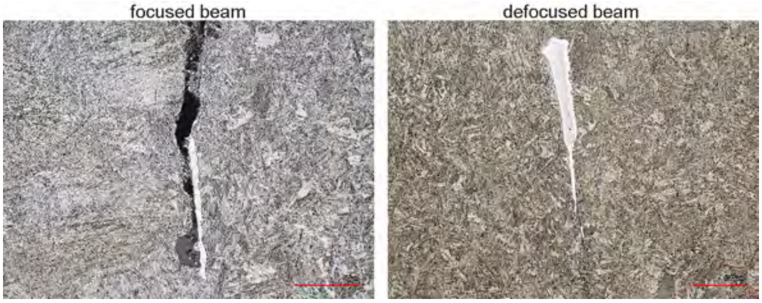

Fig. 5. Defects present on the fusion line of the weld made with the focused beam (scale 50 µm) and in the WM of the weld made with the defocused beam (scale 100 µm).

3.3. Static tensile test

The 0.2% proof strength and the ultimate tensile strength (UTS) of the base metal (BM) in the hot-stamped condition were (1120 ± 8) MPa and (1417 ± 17) MPa, respectively. The elongation at maximum load and total elongation reached (2.6 ± 0.2) % and (3.4 ± 0.3) %, respectively. Fig. 6 presents the tensile characteristics measured for both the BM and the welded joints. At least 3 specimens of each weld were tested. The welds made with beam oscillation reached a little higher average total elongation. The lower standard deviations calculated for both measured quantities of these welds indicate a more reliable weld joint.

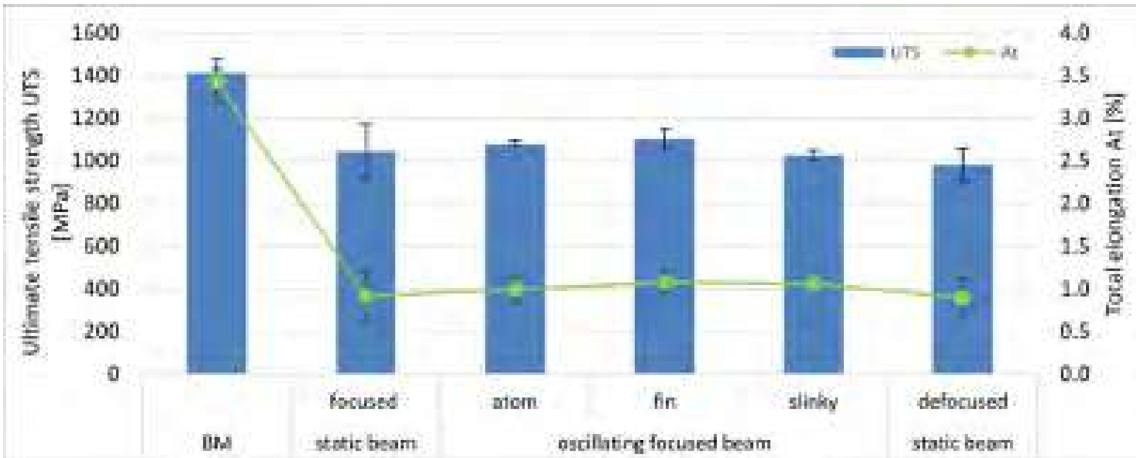

Fig. 6. Tensile characteristics of base metal and laser welds (error bars represent the standard deviation)

On the other hand, the local internal pores were detected in the laser weld made with a non-oscillating focused beam. In the case of pores present in the WM, the UTS dropped individually to only 830 MPa.

Excluding the specimens with pores, the UTS of this weld was comparable to the weld made with the fin oscillation mode. The weld made with the defocused beam reached minimal UTS resulting from a lower cooling rate promoting the higher content of bainite in bainitic-martensitic WM. The slinky mode led to the weakest joint within the welds made with beam oscillation. However, according to the standard deviations, all the welds are on a comparable level. The average values decrease in UTS and total elongation of welds towards the BM was 26 % and 71 %, respectively.

Fig. 7 presents examples of fractured specimens, two of each weld. The weld made with the focused beam fractured in the WM at low UTS, while the specimens free of pores broke in the HAZ reaching the higher UTS. Similar behavior was discovered in the weld made with the defocused beam. Besides the pores, cracks in ferritic axial segregations were observed in this weld.

The weld made with slinky oscillation mode was the only one that always fractured in the HAZ. In the case of atom oscillation mode, the solid islands were preserved in the WM, and close to them local ferritic bands were formed. One specimen fractured in this region, the other in the HAZ. The fin oscillation mode specimens fractured either in the inter-critical HAZ (ICHAZ) or the crack propagated in the coarse-grained HAZ (CGHAZ) across the arcs of WM. The specimens that broke in the HAZ reached a few dozens of MPa higher UTS. The microstructure of these zones is very similar. Beam-oscillation welds were almost free of pores. The root pores were detected only on the weld made with atom oscillation mode.

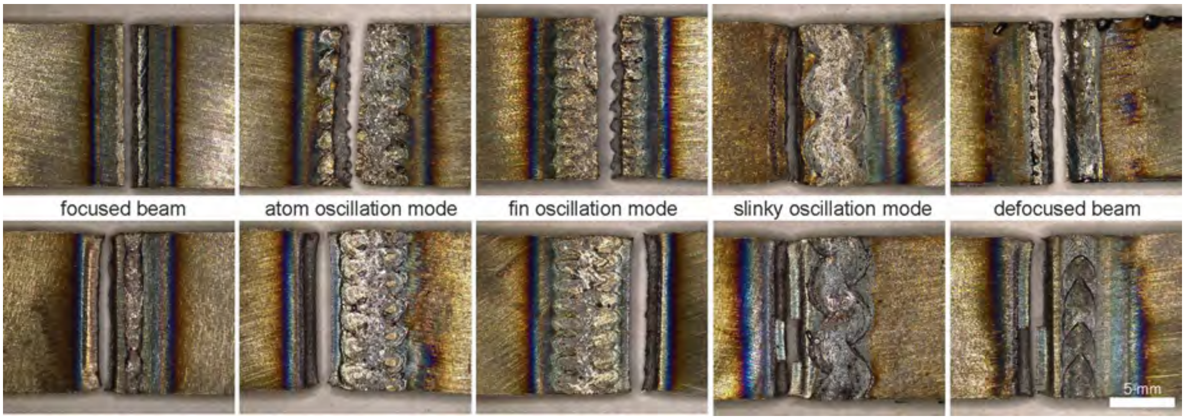

Fig. 7. Examples of fractured tensile specimens

3.4. Vickers microhardness

The BM microhardness was (477 ± 12) HV0.05. The weld metal of laser weld made with a non-oscillating focused beam reached an average microhardness of (558 ± 41) HV0.05. On the other hand, the oscillation mode atom led to the average WM microhardness of (487 ± 23) HV0.05, i.e. comparable to the BM. Fig. 8 presents the typical microhardness profile measured across this weld. The face and root results are comparable. The peak values correspond to the coarse-grained subzone of the HAZ (CGHAZ). The minimal values of microhardness are measured on the interface of ICHAZ and the sub-critical part of the HAZ (SCHAZ). The ICHAZ is the last recognizable (blue/grey-etched) zone in Fig. 3. It consists of a tempered BM and newly formed bainite/ferrite, while only a tempered BM is in the SCHAZ. The tensile test specimens broke in this area unless they broke in the FZ because of internal defects. The microhardness of WM of the weld made with a defocused beam was (491 ± 13) HV0.05, also comparable to the BM microhardness.

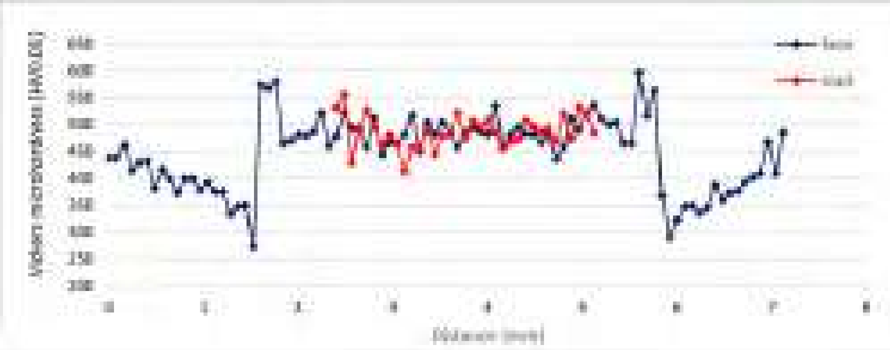

Fig. 8. Microhardness of weld made with atom oscillation mode measured 0.2 mm under the face and root surface

4. Conclusion

Laser welds made with focused and defocused beam were compared to the welds made with three different advanced oscillation modes. Contrary to the static beam, laser welds made with beam oscillation were almost free of internal defects and reached deeper penetration compared to the weld made with the defocused beam. The welds had much narrower HAZ on the face side thanks to the locally rapid spot speed. However, it widened in the root and the areas accumulating the heat thanks to the multiple beam passes.

The average microhardness of WM of laser weld made with the focused beam was about 17 % higher compared to the BM microhardness because of faster cooling compared to the hot stamping. On the other hand, the weld made with atom oscillation mode reached surprisingly lower microhardness, comparable to the BM. The high spot speed (Fig. 1) indicates low actual heat input leading to high cooling rates, and the hard fully martensitic structure of solidified weld metal can be expected after the first pass. However, the complex beam trajectory causes multiple passes increasing the heat input per unit weld length. Besides, the oscillating beam thermally affects the already solidified bead. Both reduce the resulting microhardness. Nevertheless, the highest drop of microhardness was observed on the ICHAZ/SCHAZ interface irrespective of welding technology.

The shape of the ICHAZ did not significantly affect the mechanical properties of the weld. The UTS of all welds was about the same. However, the lower standard deviations calculated for both the UTS and total elongation of welds made with beam oscillation indicate more reliable weld joints with less defects in the WM.

Acknowledgments

This work was supported by the Technology Agency of the Czech Republic [grant number FW01010293]; the Academy of Sciences of the Czech Republic [Strategy AV21 “Light in the service of society”]; and the University of Defense [Project for the development of the organization “DZRO Military autonomous and robotic systems”]. The institutional support RVO:68081731 is gratefully acknowledged.

References

Gomez, M., Garcia, C. I., Haezebrouck, D. M., Deardo, A. J., 2009. Design of composition in (Al/Si)-alloyed TRIP steels. ISIJ International 49, pp. 302–311.

Hao, K., Li, G., Gao, M., Zeng, X., 2015. Weld formation mechanism of fiber laser oscillating welding of austenitic stainless steel. Journal of Materials Processing Technology 225, pp. 77–83.

Horník, P., Šebestová, H., Novotný, J., Mrňa, L., 2022. Laser beam oscillation strategy for weld geometry variation. Journal of Manufacturing Processes 84, pp. 216–222.

Jiang, Z., Chen, X., Li, H., Lei, Z., Chen, Y., Wu, S., Wang, Y., 2020. Grain refinement and laser energy distribution during laser oscillating welding of Invar alloy. Materials & Design 186. p. 108195.

Šebestová, H., Horník, P., Mikmeková, Š., Mrňa, L., Doležal, P., Novotný, J., 2021. Microstructural characterization of laser weld of hot-stamped Al-Si coated 22MnB5 and modification of weld properties by hybrid welding. Materials 14, p. 3943.

Yan S., Meng Z., Chen B., Tan C., Song X., Wang G., 2022. Prediction of temperature field and residual stress of oscillation laser welding of 316LN stainless steel. Optics & Laser Technology 145, p. 107493.